RES MILITARIS
REVUE EUROPEENNE D ETUDES EUROPEAN JOURNAL OF MILITARY STUDIES
Social Science Journal

Flowrate Simulator with Variation of Input Voltage Based on Web Interface for Virtual Laboratory

By

Safira Firdaus Mujiyanti
Instrument Engineering, Institut Teknologi Sepuluh Nopember, Surabaya, Indonesia, 60111

Ahmad Fauzan Adziimaa
Instrument Engineering, Institut Teknologi Sepuluh Nopember, Surabaya, Indonesia, 60111

Nanda Eko Cahyo Saputra
Instrument Engineering, Institut Teknologi Sepuluh Nopember, Surabaya, Indonesia, 60111

Fadhil Nur Ahmadi
Instrument Engineering, Institut Teknologi Sepuluh Nopember, Surabaya, Indonesia, 60111

Sada Annisa Fadia
Instrument Engineering, Institut Teknologi Sepuluh Nopember, Surabaya, Indonesia, 60111

Tiffany Rachmania Darmawan
Instrument Engineering, Institut Teknologi Sepuluh Nopember, Surabaya, Indonesia, 60111

Abstract

Covid-19 requires students to conduct teaching and learning activities online or online. To help ITS instrumentation engineering students can carry out practicum activities online. Dimmer components are used to provide variations in the input voltage on the pump, so that the rotation speed of the pump can change according to the input voltage received. There are 2 flowrate sensors used to determine the flow speed produced by the pump and rotameter components used as flowrate sensor calibrators. The results of both flowrate sensors will be compared to the level of measurement accuracy. In the tool there is also a current and voltage sensor that is used to determine the input current and voltage output from the pump. Based on the tool testing that has been carried out, the pump on the tool can rotate at least receiving a current of 0.38 mA and a voltage of 154.89 V. At 80% dimmer rotation, the resulting voltage and current values have reached a maximum of 0.51 mA and 220, 3 V. The value of the current, voltage, and flowrate sensors is directly proportional to the amount of rotation of the dimmer that is set. The greater the rotation of the dimmer, the greater the value of all sensors and vice versa. In addition, the accuracy value of the YF-S201 sensor is 95.01%, YF-B1 = 97.36%, ZMPT101b = 77.08% and the ACS712 sensor is 75.09%. The flowrate sensor type YF-B1 has a higher accuracy value when compared to the flowrate sensor type YF-S201.

Keywords– Dimmer, Flowrate Simulator, Pump 1 Phase, Virtual Lab, Web Interface

Introduction

currently, the problem that Indonesia is still facing is the existence of the COVID-19 virus [1]. The COVID-19 virus can cause people's activities to be limited [2]. Students are required to carry out all online learning activities, such as practicum, internships, community service, online teaching, and learning activities. The online method is expected to break the chain of the spread of Covid 19 [3]. In supporting practicum activities, students need practicum

tools or devices that can be controlled remotely [4]. There are still many Indonesian people who are still infected with the COVID-19 virus as many as 4,255,268 people have been confirmed as COVID-19 patients [5].

Based on these problems, a solution was created by creating a tool that can be controlled remotely. According to existing research, namely Volume Design, Turbidity and PDAM Water Bill Measurement and Monitoring Systems [6]. The researcher explained that the tool contained 3 water flow sensors to calculate the flowing water discharge and 2 types of turbidity sensors were used to measure water turbidity [7]–[9]. There is also a motor that is useful for moving the existing fluid [10]. The pump can only be turned on/off so the user cannot control the rotation of the motor on the pump [11]. Controlling the rotation of the motor can reduce the starting current and reduce vibration and mechanical shock at the start [12]. In addition, this research is also used to calculate the cost of PDAM water bills based on the debit measured by the flow rate sensor [13].

The research being carried out is to design and manufacture a water measurement tool using a discharge sensor equipped with a web interface [14]. Creating a web interface aims to monitor and control the device remotely [15]. In this study, the rotation of the pump motor will be controlled using voltage variations. The rotation of the pump motor is carried out using an additional component of the AC Light Dimmer Module [16]. If the received voltage is low, the motor rotation at the pump is slow, and vice versa if the received voltage is high, the motor rotation becomes fast. The tool is also equipped with ZMPT 101B and ACS712 as current and voltage sensors and The flow rate sensors used are YF-B1 and YF-S201 with a pulse sensor type. The use of sensors aims to monitor the current and voltage used by the pump to operate [17].

Method

Measurement Block Diagram

One of the purposes of this tool is to support virtual laboratories. This tool is designed to be operated by the user from any location, without having to be near or in the area where the tool is placed. In this tool there are 4 sensors, namely a voltage sensor, a current sensor, and two flow velocity sensors. The results of 2 flow velocity sensors will be compared, which sensor has a high level of accuracy and has a value that is in accordance with the calibrator [18]. Meanwhile, current and voltage sensors are used to compare the current entering the pump with the output voltage from the pump [19].

Dimmer is a component that is used to regulate the rotational speed of the motor on the pump by adjusting the input voltage to the pump [20]. A measurement system design requires a basic system such as a measurement block diagram [21].

Measurement is one way for an observer to find out parameters/variables that are not yet known by the observer [22]. In a measurement system there are several elements in it, such as sensing elements, conditioning elements, signal processing elements, and data presentation elements [23]. The block diagram will explain the required variables and instruments [24]. Figure 1 is a block diagram of the measurement on the tool to be made.

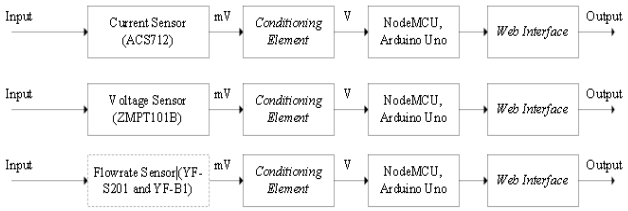

Figure 1. *Measurement Block Diagram*

Figure 1 is a measurement block diagram in this final project. One example is the first metering block diagram for measuring the input current to the pump [25]. The current that will enter the pump will be measured by the ACS712 sensor [26], then the output from the sensor will enter the conditioning element. The conditioning element will condition the output of the sensor so that it can be read or received by the microcontroller (Arduino) [27]. The signal that enters the Arduino will be processed so that the signal value can be presented to the display element [28]. This display element is used to make it easier for observers to know the current value measured by the sensor [29].

Hardware Design

The design of this hardware has several stages as follows:

1). Design hardware
2). Making electronic circuits from several components used
3). Integration several tools and component

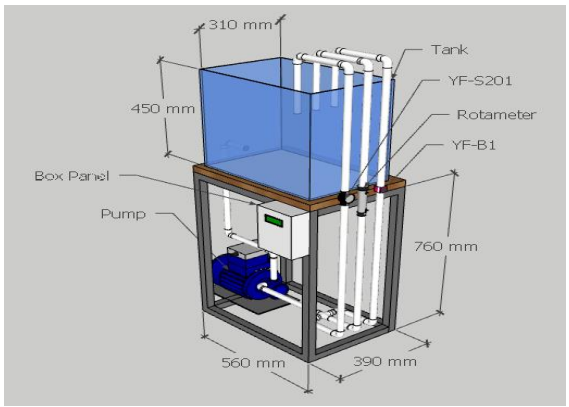

Figure 2. *Design 3D Hardware*

Figure 2 is a 3D drawing of the tool that will be made with a frame dimension of high 0.7 m and wide 0.5 m. Figure 3 is a picture of an electronic circuit that will be integrated into the device

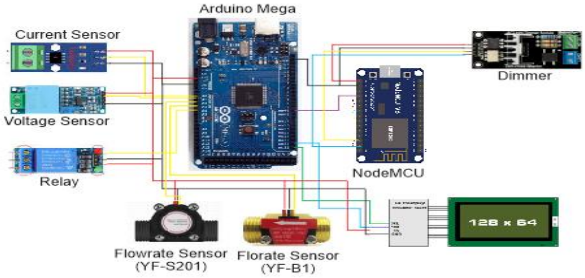

Figure 3. *Electonic Circuit*

Figure 3 is a picture of the wiring of electronic components that will be used in hardware [30]. The following are the components that will be used:

1. Arduino Uno
2. NodeMCU
3. AC Light Dimmer Module
4. Current Sensor (ACS712)
5. Voltage Sensor (ZMPT101b)
6. Flowrate Sensor (YF-S201)
7. Flowrate Sensor (YF-B1)
8. LCD 128 x 64

Results And Discussion

In the test results, several tests were carried out, namely testing the ACS712 sensor, testing ZMPT101b sensor, testing flowrate sensor, testing the prototype and the results of the monitoring design.

Current Sensor Testing (ACS712)

The current sensor (ACS712) is used to detect the current flowing in the pump. The ACS712 sensor has a measurement range between 0 - 5 A. Sensor testing is done by connecting the sensor to a single-phase pump with a multimeter as the calibrator. The following are the results of testing the ACS712 sensor.

Table 1. *Data of testing current sensor (ACS712)*

Time to-	ACS712 (A)	Multimeter (A)	%Error
1	0,32	0,31	3%
2	0,37	0,31	21%
3	0,32	0,31	3%
4	0,36	0,31	15%
5	0,36	0,31	15%
6	0,34	0,31	9%
7	0,37	0,31	21%
8	0,30	0,31	-3%
9	0,26	0,31	-15%
10	0,30	0,31	-3%
Total	3,295	3,100	0,629
Average	0,330	0,310	6,290%

Based on table 1, it can be seen the percentage value of the ACS712 sensor error. The error value is obtained from subtracting the measurement value with the value of the measuring instrument (multimeter). This experiment uses a pump load with an on condition with a rotation of 50%. Figure 4 is a graph of the data in the table.

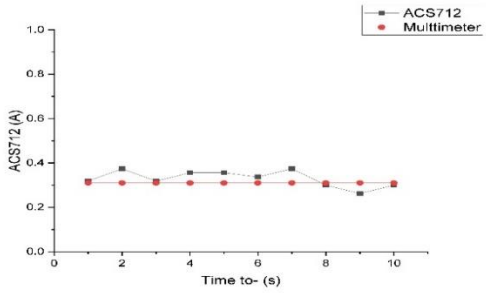

Figure 4. *Graph of Testing Current Sensor*

Figure 4 is a graph of the ACS712 sensor data in table 1. In the picture there are 2 lines, blue and red. The red line is the line from the multimeter, while the blue line is the ACS712 sensor line. The x-axis on the graph is the amount of data taken every 3 seconds, while the y-axis is the value of the ACS712 current sensor measurement. Based on the data in table 4.1, the static characteristic values of the ACS712 sensor are as follows.

Table 2. Static Characteristics of Current Sensor (ACS712)

Error		**6,29%**		
Accuracy		93,71%		
Range	0,00	-	0,37	A
Span		0,37		A

Table 2 is a table that displays the results of calculating the static characteristics of the ACS712 sensor. Based on the data in table 4.2, in pump conditions with 50% rotation the ACS712 sensor is able to detect a current at the pump of 0.37 A. With the ACS712 sensor accuracy value of 93.71%, it means that the ACS712 sensor measurement value is almost close to the measurement value. validator (Multimeter).

Voltage Sensor Testing (ZMPT101b)

ZMPT101b sensor is a sensor that is used to measure the voltage used to rotate a pump on the device. ZMPT101b sensor testing is done by connecting the ZMPT101b sensor directly to the home electricity supply. A multimeter is used to measure voltage and as a calibrator rather than a voltage sensor. Table 3 is the data from the voltage sensor test results.

Table 3. *Data of testing voltage sensor (ZMPT101b)*

Time to-	ZMPT101B (V)	Validator (V)	%Error
1	226,71	227	0,13
2	227,74	227	0,33
3	227,83	229	0,51
4	228,40	228	0,18
5	226,99	227	0,00
6	226,38	228	0,71
7	228,86	229	0,06
8	227,81	229	0,52
9	225,77	229	1,41
10	228,49	229	0,22
Total	2274,98	2282,00	4,07
Average	227,50	228,20	0,41

Based on table 3, it can be seen the percentage error value of the ZMPT101B sensor where the error value is obtained from subtracting the measurement value with the value of the measuring instrument (multimeter). Data collection in table 3 is done by connecting the ZMPT101b sensor to the electricity supply. The ZMPT101b sensor data retrieval was carried out 10 times per 3 seconds. From the data in table 3. can be displayed graph as shown in Figure 5. namely the graph of the relationship between the ZMPT101b sensor and the validator (multimeter).

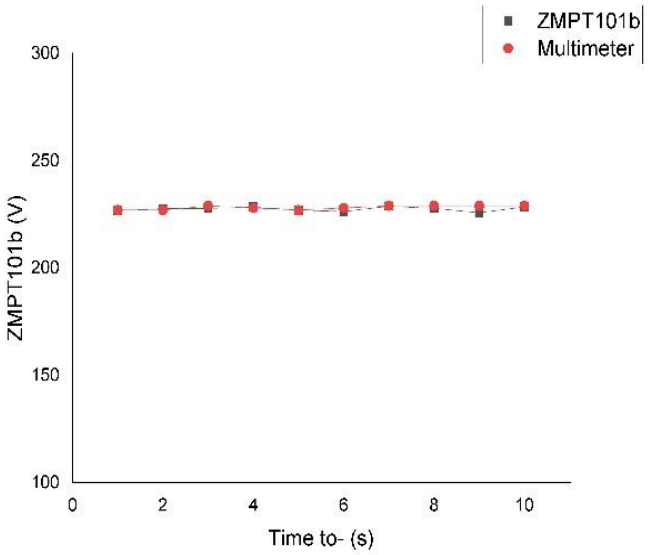

Figure 5. *Graph of Testing Voltage Sensor (ZMPT101b)*

Figure 5 is a graph of the ZMPT101B sensor data in table 3. In the picture there are 2 lines, blue and red. The red line is the line from the multimeter, while the blue line is the line from the ZMPT101B sensor. The x-axis on the graph is the amount of data taken every 3 seconds, while the y-axis is the value of the ZMPT101B current sensor measurement. Based on the data in table 3, the static characteristic values of the ZMPT101b sensor are as follows.

Table 4. *Static Characteristics of Voltage Sensor (ZMPT101b*

Error		**0,31%**		
Accuracy		99,69%		
Range	0,00	-	228,86	V
Span		228,86		V

Table 4 is a table that displays the results of calculating the static characteristics of the ZMPT101b sensor. Based on the data in table 4, in the condition of the ZMPT101b sensor, the sensor connected to electricity can detect a voltage of 228.86 A. With the ZMPT101b sensor accuracy value of 99.69%, the ZMPT101b sensor has a value close to the validator measurement value with an error value the average is 0.31%.

Flowrate Sensor Testing (YF-S201)

Testing the YF-S201 sensor is carried out directly on a hardware device that has been assembled. The flowrate sensor is installed parallel to the rotameter. The rotameter is used as a calibrator rather than a flowrate sensor (YF-S201). Table 5 is the test data for the YF-S201 sensor and Figure 6 is a graph of the test data.

Table 5. *Data of testing flowrate sensor (YF-S201)*

Time To-	YF-S201 (LPM)	Rotameter (LPM)	%Error
1	3,04	2,80	8,57%
2	3,00	2,80	7,14%
3	2,95	2,80	5,36%
4	3,18	2,80	13,57%
5	2,89	2,80	3,21%
6	2,80	2,80	0,00%
7	2,74	2,80	2,14%
8	2,84	2,80	1,43%
9	2,84	2,80	1,43%
10	2,71	2,80	3,21%
Total	28,990	28,000	0,461
Average	2,899	2,800	4,61%

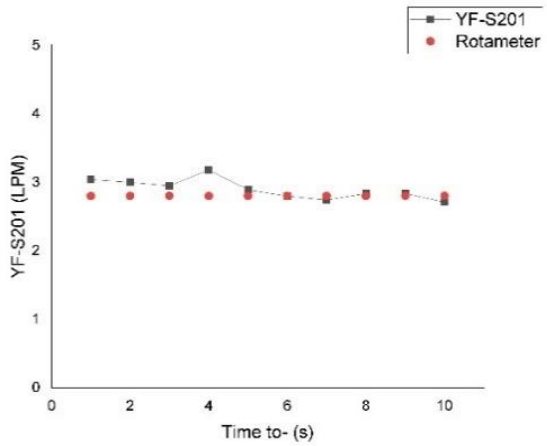

Figure 6. *Graph of Testing Flowrate Sensor (YF-S201)*

Figure 6 is a graph of the YF-S201 sensor data in table 5. In the picture there are 2 lines, blue and red. The red line is the result of measurements from the rotameter, while the blue line is the line from the YF-S201 sensor. The x-axis in the graph is the amount of data taken every 3 seconds, while the y-axis is the value of the YF-S201 current sensor measurement in LPM units. Based on the data in table 6, the value of the static characteristic of the YF-S201 sensor is as follows.

Table 5. Static Characteristics of Flowrate (YF-S201)

Error			**3,54%**	
Accuracy			96,46%	
Range	0,00	-	3,18	LPM
Span		3,18		LPM

Flowrate Sensor Testing (YF-B1)

Testing the YF-B1 sensor is carried out in the same way as the YF-S201 sensor. The flowrate sensor is installed parallel to the rotameter. The rotameter is used as a calibrator rather than a flowrate sensor (YF-B1). Table 7 is the test data for the YF-B1 sensor and Figure 7 is a graph of the test data.

Table 7. *Data of testing flowrate sensor (YF-B1)*

Time to-	YF-S201 (L/M)	Rotameter (LPM)	%Error
1	3,02	2,80	7,86%
2	2,93	2,80	4,64%
3	2,83	2,80	1,07%
4	2,89	2,80	3,21%
5	2,81	2,80	0,36%
6	2,86	2,80	2,14%
7	2,79	2,80	0,36%
8	2,80	2,80	0,00%
9	2,83	2,80	1,07%
10	2,83	2,80	1,07%
Total	28,590	28,000	0,218
Average	2,859	2,800	2,179%

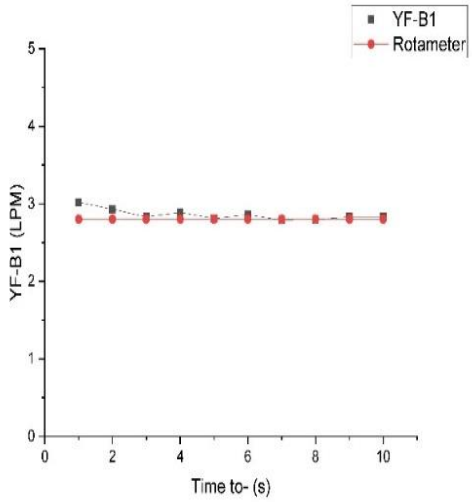

Figure 7. *Graph of Testing Flowrate Sensor (YF-B1)*

Figure 7 is a graph of the YF-B1 sensor data in table 7. In the picture there are 2 lines, blue and red. The red line is the result of the measurement from the rotameter, while the blue line is the line from the YF-B1 sensor. The x-axis on the graph is the amount of data taken every 3 seconds, while the y-axis is the value of the YF-B1 current sensor measurement in LPM units. Based on the data in table 8, the value of the static characteristic of the YF-B1 sensor is as follows.

Table 6. *Static Characteristics of Flowrate (YF-S201)*

Error			2,11%	
Accuracy			97,89%	
Range	0,00	-	3,02	LPM
Span		3,02		LPM

Hardware Testing

Hardware testing is the next procedure after integrating all components. Testing of this tool is carried out to determine the performance of the tool that has been designed. Table 9 is the measurement data from the current, voltage, and flowrate sensors that have been integrated into the tool.

Table 7. *Summary of Measurement Data When Testing Hardware*

Dimmer (%)	YF-S201 (LPM)	YF-B1 (LPM)	Rotameter (LPM)	ACS712 (mA)	Multimeter (mA)	ZMPT101B (V)	Multimeter (V)
45	1,90	1,85	1,76	0,31	0,32	231,96	156,40
50	1,93	2,06	2,10	0,52	0,38	230,72	173,50
60	2,18	2,25	2,30	0,36	0,43	230,27	198,20
70	2,53	2,53	2,50	0,29	0,48	215,70	213,60
80	2,79	2,782	2,7	0,488	0,51	212,202	220,30

Table 9 is a table of sensor measurement data at the time of testing the hardware. Each data dimmer condition is taken as much as 10 data per 3 seconds. In table 9 there is data all sensors used like, current, voltage, flowrate, rotameter, and multimeter sensors. The data shown in table 9 is the average value of each measurement condition. Based on the data in table 9, it can be seen the characteristics of the sensor at the time of testing and the graph of the sensor value.

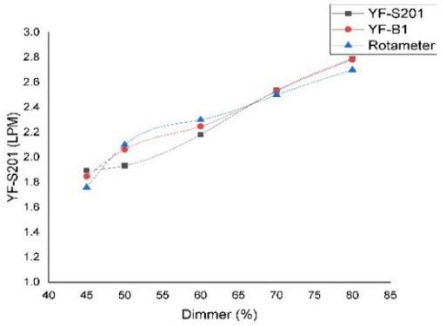

Figure 8. Graph of Relationship Between Flowrate Sensor Value and Rotameter

Based on Figure 8, the value of the flow velocity on the two sensors, namely the YF-S201 and YF-B1 sensors, is in the same direction (linear) as the value measured by the rotameter. The following are static characteristics obtained from table 9.

Table 8. *YF-S201 Sensor Static Characteristics During Hardware Testing*

Error			**4,99%**	
Accuracy			95,01%	
Range	0,00	-	2,89	LPM
Span		2,89		LPM

Table 9. *YF-B1 Sensor Static Characteristics During Hardware Testing*

Error			**2,64%**	
Accuracy			97,36%	
Range	0,00	-	2,81	LPM
Span		2,81		LPM

Based on the data in tables 10 and 11 the flowrate sensor with the YF-B1 type has a higher accuracy value than the YF-S201 sensor with the YF-S201 sensor accuracy value is 95.01% while the YF-B1 sensor is 97.36%. Figures 8 and 9 are graphs for the ZMPT101b sensor and the ACS712 sensor.

Data collection in Table 7 was carried out as many as 5 pump rotation conditions, namely 45%, 50%, 60%, 70%, and 80%. Data retrieval was carried out simultaneously as many as 10 data taken in each difference in the dimmer round. Based on the data in table 4.9 it can be known that at a turn of 35%-60% the value of the water flow rate changes significantly, while at a turn of 60%-80% the value of the water flow rate does not change significantly. This can happen because the voltage value obtained from 60%-80% has a small difference when compared to the voltage difference at 35%-60% rotation.

Data collection is carried out starting from a 45% dimmer rotation because when the dimmer rotation is set at 35% rotation, the pump turns on but water cannot re-enter the tank. This happens because the current value and voltage value entering the pump do not meet the minimum current and voltage limits of the pump. Based on the test results, the rated voltage generated at the 35% dimmer rotation is 93.9 V. So the minimum limit to be able to rotate the pump so that it can pump water back into the container is 45%. In addition, the cause of the pump not being able to rotate is one of which is that there is a scale that settles inside the pump motor.

At the time of the dimmer is set at a rotation of 80% the voltage and current read by the multimeter is 220.3 V and 0.51 mA. Meanwhile, when the pump is set with a rotation of 81%-90% the sensor and rotameter experience unstable data readings. In addition, the rotation of the pump decreases. Based on the tool testing that I have done at the time when the dimmer rotation is set by 90% the voltage read by the multimeter is 173.1 V.

The relationship between voltage sensor and dimmer rotation shows in Figure 7.

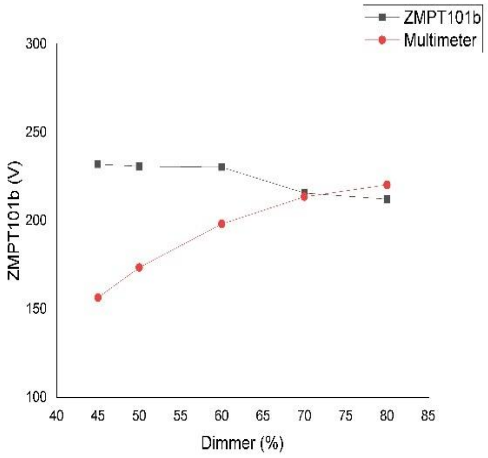

Figure 7. *Graph of Relationship Between Voltage Sensor with Dimmer*

Based on Figure 9, the ZMPT101b sensor value is directly proportional (linear) to the percentage of dimmer rotation. The greater the dimmer value, the higher the value measured by the ZMPT101b sensor. That graph shows the relationship between the voltage sensor and the dimmer rotation. The x-axis on the graph is the dimmer rotation with a percent unit (%), while for the y-axis it is the value of the voltage sensor with a volt unit (V). Similarly, when data retrieval on the flowrate sensor, the rotation of the dimmer is set from 30% to 85%. Based on figure 4.8, the ZMPT101b sensor reading has a far measurement value when compared to the multimeter reading value because the input voltage division on the sensor is uneven. At a dimmer turn of 40% to 60% the measurement value of the ZMPT101b sensor with a multimeter has a much different value. The farthest difference is in the 45% dimmer round. Where the measurement value of the ZMPT101b sensor at the time of 45% rotation is 231.96 V while the

multimeter reading at 45% rotation is 156.40 V. At the dimmer rotation 70% the sensor value of ZMPT101b and the multimeter is almost close, where the sensor value of ZMPT101b is 215.70 V while the multimeter reading is 213.60 V. Dimmer rotation is 80% the difference in the measurement value of the ZMPT101b sensor with the multimeter is approximately 8.10 V. Where the sensor value of ZMPT101b is 212.20 V while the measurement value is multimeter 220.30 V. Table 12 is the characteristic value obtained from the measurement results of the ZMPT101b sensor in table 9.

Table 12. *ZMPT101b Sensor Static Characteristics During Hardware Testing*

Error		**20%**		
Accuracy		80%		
Range	0,00	-	235,01	V
Span		235,01		V

Based on table 12, the accuracy value of the ZMPT101b sensor decreases when compared to the accuracy value of the ZMPT101b sensor when the sensor is validated.

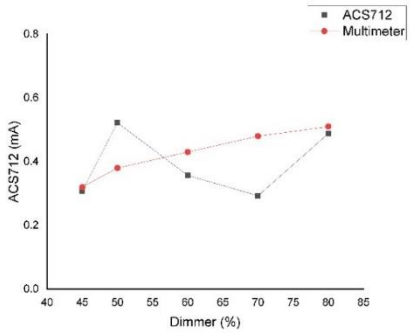

Figure 8. *Graph of Relationship Between Current Sensor Value with Round of Dimmer*

Based on Figure 10, the ACS712 sensor value is directly proportional (linear) to the dimmer percentage value and voltage value. The following is a table of the static characteristics of the ACS712 sensor when testing the hardware.

Table 10. *ACS712 Sensor Static Characteristics During Hardware Testing*

Error		**20%**		
Accuracy		80%		
Range	0,00	-	1,01	mA
Span		1,01		mA

Based on table 13 the ACS712 sensor accuracy value has decreased when compared to the ACS712 sensor value at the time of sensor validation.

That result shows the relationship between the current sensor and the dimmer rotation. The x-axis on the graph is the dimmer rotation with a percent unit (%), while for the y-axis it is the value of the current sensor with an ampere unit (mA). Unlike the ZMPT101b sensor, this ACS712 current sensor has almost the same measurement value at the time of 45% and 80% dimmer rotations. However, at the dimmer rotation of 50% to 75% has a significant difference in measurement. Based on figure 4.9, the current measurement value is significantly different at a dimmer rotation of 70% with the measurement value of the ACS712 current sensor is 0.29 mA while the current measurement on the multimeter is 0.48 mA. For measurements of values that are almost close to validators, there is a dimmer rotation of 45% with the value of the

ACS712 sensor is 0.31 mA while the current measurement on the multimeter is 0.32 mA and at the dimmer rotation of 80% with the current value on the ACS712 sensor is 0.48 mA while the value read on the multimeter is 0.51 mA.

Conclusion

The conclusions that can be seen from the results of the discussion in chapter 4 are as follows:

a. Based on the test data, the value of voltage, current, and water flow velocity produced by each sensor is directly proportional. The greater the rotation of the dimmer, the greater the value of current, voltage and flowrate.
b. The accuracy value of each sensor decreases when testing the tool, where the accuracy value of the YF-S201 sensor is 95.01%, YF-B1 = 97.36%, ZMPT101b = 80% and the ACS712 sensor is 80%. Based on the accuracy value, the YF-B1 sensor has a higher accuracy rate when compared to the YF-S201 sensor.

Acknowledgements

We would like to appreciate the support provided from Instrumentation Engineering Department, Sepuluh Nopember Intitute of Technology for providing allocation for this work and collaborative effort.

References

R. Syamsuddin, U. N. Makassar, and D. Pandey, “Corana Pandemic (Covid-19) and Interdisciplinary Issues,” no. December, 2020.
ECLAC, “The effects of the coronavirus disease (COVID-19) pandemic on international trade and logistics,” United Nation ECLAC, no. 6, p. 7, 2020, [Online]. Available: https://www.cepal.org/en/publications/45878-effects-coronavirus-disease-covid-19-pandemic-international-trade-and-logistics.
M. J. Lubis and L. P. Sari, “The Online Learning Activities during the Covid 19 Pandemic,” Budapest Int. Res. Critics Inst. Humanit., vol. 3, no. 4, pp. 3619–3624, 2020.
F. V. De Almeida et al., “via a Remote Lab,” 2022.
S. Asia, “Covid-19 Response Fund Western Pacific Data More Resources Americas Covid-19 Response Fund Western Pacific,” pp. 1–5, 2022.
C. Widiasari and L. Anugrah Zulkarnain, “Rancang Bangun Sistem Monitoring Penggunaan Air PDAM Berbasis IoT,” J. Komput. Terap., vol. 7, no. Vol. 7 No. 2 (2021), pp. 153–162, 2021, doi: 10.35143/jkt.v7i2.5152.
T. Uchiyama, K. Takamure, Y. Okuno, and E. Sato, “Development of a self-powered wireless sensor node to measure the water flowrate by using a turbine flowmeter,” Internet of Things (Netherlands), vol. 13, p. 100327, 2021, doi: 10.1016/j.iot.2020.100327.
H. Li, Y. Liu, K. Li, J. Deng, Y. Feng, and J. Liu, “A resonant piezoelectric proportional valve for high-flowrate regulation operated by a bending sandwich actuator,” Sensors Actuators, A Phys., vol. 331, p. 112971, 2021, doi: 10.1016/j.sna.2021.112971.
H. Wang, M. Zhang, and Y. Yang, “Machine learning for multiphase flowrate estimation with time series sensing data,” Meas. Sensors, vol. 10–12, no. November, p. 100025, 2020, doi: 10.1016/j.measen.2020.100025.
United States Department of Energy (DOE), “Module 3: Pumps,” DOE Fundam. Handb. Mech. Sci. Vol. 1 2, no. 3923, pp. 1–28, 1993.

S. M. Abelin, “Improving Pumping System Performance,” U.S. Dep. Energy, p. 117, 2006.
Y. Xie, C. Pi, and Z. Li, “Study on design and vibration reduction optimization of high starting torque induction motor,” Energies, vol. 12, no. 7, 2019, doi: 10.3390/en12071263.
P. During, “Suction check of very small workpieces,” pp. 947–969.
H. El-Bakry et al., “Adaptive User Interface for Web Applications,” 4th WSEAS Int. Conf. Bus. Adm. (ICBA ’10), no. October, pp. 190–211, 2010.
I. J.-K. Trzeciak Mateusz, “Effectiveness Drivers in Polish Energy Sector . Diagnosis and,” 2021.
A. Sani and E. E. N. Jannah, “Purwarupa Pengendali Kecepatan Motor Induksi 1 Fasa Via Android,” J. Integr., vol. 12, no. 2, pp. 88–91, 2020, doi: 10.30871/ji.v12i2.2016.
M. M. Werneck, “Current and Voltage Sensing,” Plast. Opt. Fiber Sensors, no. March, pp. 107–129, 2019, doi: 10.1201/b22357-5.
Q. Quan, “Introduction to multicopter design and control,” Introd. to Multicopter Des. Control, no. February, pp. 1–384, 2017, doi: 10.1007/978-981-10-3382-7.
J. S. A, A. K. A, and Y. A. M, “Development of A Water-Pump Control Unit with Low Voltage Sensor,” Int. J. Energy Eng., vol. 2015, no. 2, pp. 34–39, 2015, doi: 10.5923/j.ijee.20150502.03.
A. Fitriani and G. Wang, “Examining the Security Issues related to ATM use with Revised TAM,” Telkomnika, vol. 13, no. 2, 2015, doi: 10.12928/TELKOMNIKA.v13i2.xxxx.
A. Neely et al., “Performance measurement system design: Developing and testing a process-based approach,” Int. J. Oper. Prod. Manag., vol. 20, no. 10, pp. 1119–1145, 2000, doi: 10.1108/01443570010343708.
Jane, “Chapter 5 Measurement Operational Definitions Numbers and Precision Scales of Measurement Validity of Measurement Content Validity,” pp. 5–16, 2016.
S. S. Generator, “Benha University Faculty of Engineering at Shubra Electrical Engineering Department Electric Machines II,” pp. 1–23.
C. N. On, “Class Notes on Electrical Measurements & Instrumentation,” 2015.
M. A. Haidekker, “Block diagrams: formal graphical description of linear systems,” Linear Feed. Control., pp. 123–131, 2020, doi: 10.1016/b978-0-12-818778-4.00016-9.
M. Taif, M. Y. Hi. Abbas, and M. Jamil, “Penggunaan Sensor Acs712 Dan Sensor Tegangan Untuk Pengukuran Jatuh Tegangan Tiga Fasa Berbasis Mikrokontroler Dan Modul Gsm/Gprs Shield,” PROtek J. Ilm. Tek. Elektro, vol. 6, no. 1, 2019, doi: 10.33387/protk.v6i1.1009.
A. S. Ismailov and Z. B. Jo‘rayev, “Study of arduino microcontroller board,” "Science Educ. Sci. J., vol. 3, no. 3, pp. 172–179, 2022.
M. A. Al-yoonus, “Understanding the concept of data acquisition using Arduino Introduction :,” no. February, pp. 1–5, 2020, doi: 10.13140/RG.2.2.12699.62245.
S. Ziegler, R. C. Woodward, H. H. C. Iu, and L. J. Borle, “Current sensing techniques: A review,” IEEE Sens. J., vol. 9, no. 4, pp. 354–376, 2009, doi: 10.1109/JSEN.2009.2013914.
K. Chen, J. Wang, and S. Jiao, “The management and applications of shield machines (TBM),” Shield Constr. Tech. Tunneling, pp. 485–551, 2021, doi: 10.1016/b978-0-12-820127-5.00010-1.